LBNL-45465
Preprint

ERNEST ORLANDO LAWRENCE
BERKELEY NATIONAL LABORATORY

Osmotic Second Virial Cross Coefficients for Star and Linear Polystyrenes

Alberto Striolo and John M. Prausnitz

Chemical Sciences Division

April 2000

Submitted to
Journal of Chemical Physics

REFERENCE COPY
Does Not
Circulate

Bldg. 50 Library - Ref.
Lawrence Berkeley National Laboratory

LBNL-45465

Copy 1

DISCLAIMER

This document was prepared as an account of work sponsored by the United States Government. While this document is believed to contain correct information, neither the United States Government nor any agency thereof, nor the Regents of the University of California, nor any of their employees, makes any warranty, express or implied, or assumes any legal responsibility for the accuracy, completeness, or usefulness of any information, apparatus, product, or process disclosed, or represents that its use would not infringe privately owned rights. Reference herein to any specific commercial product, process, or service by its trade name, trademark, manufacturer, or otherwise, does not necessarily constitute or imply its endorsement, recommendation, or favoring by the United States Government or any agency thereof, or the Regents of the University of California. The views and opinions of authors expressed herein do not necessarily state or reflect those of the United States Government or any agency thereof or the Regents of the University of California.

LBNL-45465

Osmotic Second Virial Cross Coefficients for Star and Linear Polystyrenes

Alberto Striolo and John M. Prausnitz
Department of Chemical Engineering
University of California
and
Chemical Sciences Division
Lawrence Berkeley National Laboratory
University of California
Berkeley, CA 94720, U.S.A.

April 2000

This work was supported by the Director, Office of Science, Office of Basic Energy Sciences, Chemical Sciences Division of the U.S. Department of Energy under Contract Number DE-AC03-76SF00098.

Osmotic Second Virial Cross Coefficients for Star and Linear Polystyrenes

Alberto Striolo[a] and John M. Prausnitz*

Chemical Engineering Department, University of California, Berkeley

and

Chemical Sciences Division

Lawrence Berkeley National Laboratory, Berkeley, CA 94720

Abstract

Experimental osmotic second virial cross coefficients are reported for linear and 8-arm star polystyrenes in three solvents: toluene, cyclohexane and methylcyclohexane. The osmotic second virial cross coefficient for 8-arm star and linear polystyrene is always positive and within the osmotic second virial coefficients measured for the single polymers. The positive cross coefficient indicates net repulsion between the two different polymers in dilute solution. The extent of repulsion is greatest in toluene and least in cyclohexane.

To relate the macroscopic second virial coefficient to microscopic interactions, the potential of mean force between linear and 6-arm star polymers was computed by molecular simulation. The interaction between non-bonded polymer segments is given by a square-well potential. Well width was set equal to one half of the segment diameter. Different solvent conditions were investigated by using different well depths. Potentials of mean force were then used to compute the osmotic second virial cross coefficients.

Key Words: Osmotic Second Virial Coefficient; Monte Carlo Simulation; Potential of Mean Force; Radial Distribution Function.

[a] on leave from Istituto di Impianti Chimici, Università di Padova, Via Marzolo 9, I-35131 Padova, Italy

* to whom correspondence should be addressed

Introduction

The osmotic second virial coefficient is useful for describing interactions between a pair of large solute molecules in dilute solution. Light scattering and osmometry are commonly used to measure the osmotic second virial coefficient at different solvent conditions. Numerous articles have reported osmotic second virial coefficients for dissolved single polymers[1-4] and for aqueous proteins[5-7]. Only few reports have appeared for two-solute systems (see, for example, reports on the interaction between polymer and protein [8, 9], between different proteins [10], and between different polymers[8, 9]).

This work reports osmotic second virial coefficients for pairs of polymers that are chemically similar but have different architectures.

Second osmotic virial coefficients for linear and star polymers have been reported[11, 12]). Applications of mixtures of star and linear polymers are under development (see, for example, Guo et al.[13] and references therein). For example, star-linear polymer mixtures are suitable for coatings and paints[14].

Star polymers with many low-molecular-weight arms can be considered as spherical, colloidal particles[15]; colloidal dispersions are used in paints, inks, electronics, ceramics, oil recovery and bioseparations (for a detailed discussion, see Hiemenz and Rajagopalan[16]). In many of these dispersions, polymers are also present, either to enhance the stability of the dispersion (e.g. manufacture of inks and paints) or to promote separation of the colloids (e.g. protein precipitation by nonionic polymers). Efforts are in progress to understand the potential of mean force between colloidal particles in a polymer-containing solution, by theoretical calculations (for a discussion, see Yethiraj et al.[17]) or by computer simulation[18, 19]. Experimental osmotic virial cross coefficients are needed to test theoretical results.

In this work, we studied experimentally solutions of 8-arm-star and linear polystyrenes at different conditions. Solvents used were toluene, cyclohexane and methylcyclohexane. At normal experimental temperatures, toluene is a good solvent for both polymers; cyclohexane and methylcyclohexane are good solvents for star polystyrene, but they are theta and poor solvents for the linear homologue[20].

The experimental second virial coefficients provide information on overall interactions between linear and star polymer in dilute solutions. However, they do not

provide insights concerning microscopic interactions between the different polymers. Monte Carlo simulation calculations were therefore used to compute the potential of mean force for a simple model of linear and star polymers that roughly mimics the systems studied experimentally.

Materials and Experimental Method

Linear and 8-arm star polystyrenes of comparable molecular weight were used. Table 1 shows polymer properties. Polymers were kept under vacuum for a few days before use. Table 2 shows solvents characteristics; solvents were used as received. A membrane osmometer, model 231, from Jupiter Instrument Co., was used to measure the osmotic pressures of polymer solutions of different composition. The temperature was kept constant at ±0.2°C over a 12-hour period with an electric-resistance heater. Equilibration required anywhere from twenty to sixty minutes for each polymer solution. The cellulose acetate membrane had a molecular-weight-cut-off of either 10,000 or 20,000 g/mole.

For a solution of a single polymer in a solvent, the osmotic pressure, Π, is related to the polymer's number-average molecular weight, M, through:

$$\frac{\Pi}{R \cdot T} = \frac{1}{M} c + B \cdot c^2 + \ldots \quad , \qquad (1)$$

where R is the gas constant, T is the absolute temperature, c is the polymer mass concentration and B is the osmotic second virial coefficient[21]. Osmotic second virial coefficients for the single polymers were determined by fitting Equation 1 to the experimental osmotic pressures.

For a solution of two different solutes, for example star and linear polymers, the osmotic pressure is given by:

$$\frac{\Pi}{R \cdot T} = \frac{1}{M_l} c_l + B_{ll} \cdot c_l^2 + \frac{1}{M_s} c_s + B_{ss} \cdot c_s^2 + 2 \cdot B_{ls} \cdot c_l \cdot c_s + \ldots \quad , \qquad (2)$$

where B_{ls} is the osmotic second virial cross coefficient for linear and star polymers; subscripts l and s refer to linear and to star, respectively. For various Π measurements, the relative concentrations of linear and star polymers were not constant to assure that the experimental data give a 'composition-independent' osmotic second virial cross

coefficient. Π was measured for 10-15 samples of polymer solutions in each solvent. The results reported for B_{ls} are obtained by fitting to Equation 2 the experimental osmotic pressures measured at different polymer concentrations.

Experimental Results

Table 3 shows measured osmotic second virial coefficients. The osmotic second virial cross coefficient B_{ls} is always positive and lies between the osmotic second virial coefficients for the single polymers. B_{ls} is larger in toluene and smaller in cyclohexane. Repulsion between non-like polymers in methylcyclohexane is larger than that in cyclohexane. Because the polymers have the same chemistry, repulsion is probably due to the different architectures of the interacting polymers. A star polymer has a smaller radius of gyration and a higher segment density at small distances from the center of mass than those for a linear polymer of the same molecular weight (see, for example, Table 4). The star polymer is a more dense and compact molecule, compared to the linear polymer. Therefore, a star polymer cannot easily penetrate into another polymer, giving a net repulsion between the two at low separations. To understand better details of the microscopic interactions, we performed molecular-simulation calculations.

Molecular Simulation

The linear polymer is represented as a chain of either 100 ($linear_{100}$) or 200 ($linear_{200}$) freely-jointed-hard-spheres, while the star molecule is represented as six chains of 17 segments each departing from a central core. The core has the same characteristics as those of any other polymer segment. The effect of branching upon thermodynamic properties increases with rising number of arms. However, the model star polymer with six arms was detailed enough to explain the differences in theta temperature measured between linear and 8-arm star polystyrene in methylcyclohexane[20]. Therefore, we used the 6-arm-star model, for which potentials of mean force and second virial coefficients are available[20]. Different well depths were used to represent different solvent conditions, from good to poor. Dynamic Monte Carlo techniques, such as the widely adopted reptation algorithm[22, 23] are not suitable to generate equilibrium conformations of branched structures. Therefore, the Pivot algorithm[24, 25] was used to generate isolated

configurations of both linear and star polymers. To represent different solvent conditions, a square-well attraction between non-consecutive polymer segments was used. Well width was set equal to one half the segment diameter. Good solvent conditions for both polymers are represented using a well depth equal to zero, –0.15 k_BT, and –0.30, while –0.40 k_BT represents solvents better for the star polymer than for the linear homologs; k_B is the Boltzmann's constant and T is the absolute temperature. The osmotic second virial coefficient equals zero (theta condition) for a well depth equal to -0.32 k_BT for a linear polymer[26], and for a well depth equal to –0.35±0.02 k_BT for a 6-arm star polymer[20]. Because the solvent is considered as a continuum, the adopted potential between non-bonded polymer segments is considered as a solvent-mediated potential of mean force. Solvent molecular characteristics may be important, especially for hydrogen-bonding solvents. However, the continuous-solvent model offers a reasonable approximation for solutions of polymers in nonpolar solvents without preferential interactions. The algorithm here employed offers a molecular explanation for thermodynamic differences between linear and star polystyrenes in common solvents[20, 26]. The square-well potential, $\phi(d)$, between non-bonded segments is:

$$\phi(d) = \begin{cases} \infty & d < \sigma \\ \varepsilon & \sigma \le d \le 1.5 \cdot \sigma \end{cases} , \qquad (3)$$

where σ, ε, and d represent the segment diameter, the well depth and the center-to-center distance between two segments, respectively.

To calculate the potential of mean force as a function of the distance between the centers of mass of the polymers, r, we used the algorithm proposed by Hall and coworkers[26, 27] and slightly modified by Lue and Prausnitz[28]. The potential of mean force, as a function of the distance between the polymers' centers of mass, W_{ij} (r), is obtained by:

$$\frac{W_{ij}(r)}{k_B \cdot T} = -\ln \frac{\sum_{l=1}^{N} U_l(r)}{N} , \qquad (4)$$

where N is the total number of linear-star configurations used at each distance, and U_l (r) is the statistical weight of each polymer pair at given separation r. This quantity is obtained by:

$$U_l(r) = \exp^{\frac{-\Phi_l(r)}{k_B \cdot T}} \quad , \tag{5}$$

where Φ_l (r) is the potential between the two configurations. Subscripts i and j refer to the interacting polymers, either linear or star. This quantity is equal to infinity if at least one segment of one polymer overlaps with a segment of the interacting polymer. If there are no overlaps, it is equal to the number of segment pairs belonging to the two interacting polymers distant less than 1.5 times the segment diameter σ, multiplied by the well depth. 1,000 different conformations for both the linear and the star polymer were used for a total of 1,000,000 polymer pairs at each separation. Dautenhahn and Hall[26] have reported calculations of potentials of mean force between linear chains as a function of the center of mass separation and of well depth. Here we are concerned with the potentials of mean force between linear-linear, star-star and linear-star polymer pairs. The potential of mean force, computed as a function of the distance between centers of mass, r, is used to determine the osmotic second virial coefficient as a function of solvent conditions according to:

$$B'_{ij} = 2 \cdot \pi \cdot \int_0^\infty r^2 \cdot \left(1 - \exp\left[-\frac{W_{ij}(r)}{k_B \cdot T}\right]\right) \cdot dr \quad . \tag{6}$$

In Equation 6, B'_{ij} is expressed in volume units. B_{ij} and B'_{ij} are related by:

$$B_{ij} = \frac{B'_{ij} \cdot N_A}{M_i \cdot M_j} \quad , \tag{7}$$

where N_A is Avogadro's number. From the potential of mean force, it is also possible to compute the radial distribution function, g_{ij} (r), as a function of the distance r:

$$g_{ij}(r) = \exp^{\frac{-W_{ij}(r)}{k_B \cdot T}} \quad . \tag{8}$$

The results shown are the average of at least three different runs.

Table 4 shows calculated radii of gyration for all polymers at different solvent conditions. At each solvent condition, the radius of gyration for the 6-arm star polymer is smaller than that for the linear chain with the same number of segments.

Figure 1 shows the radial distribution function as a function of the distance between centers of mass for the linear_{100}-linear_{100}, star-star, and linear_{100}-star pairs at athermal conditions. The radial distribution function for the linear-star pair is always

within the radial distribution functions of the linear-linear and star-star pairs. Figure 2 shows the radial distribution function as a function of the distance between centers of mass for the $linear_{100}$-$linear_{100}$, star-star, and $linear_{100}$-star pairs for a well-depth equal to –0.40 k_BT. The radial distribution function for the $linear_{100}$-star case shows that penetration between star and linear polymer is possible, even though less probable than that between two $linear_{100}$ polymers. At distances between 5 and 10 times the segment diameter, the attractive potential between two different polymers is weaker than that between two like polymers.

Figure 3 shows the radial distribution function as a function of the distance between centers of mass for the $linear_{200}$-$linear_{100}$, and $linear_{200}$-star pairs at athermal conditions. The radial distribution function for the $linear_{200}$-star pair is lower than that for the $linear_{200}$-$linear_{100}$ pair at low separations, but higher between 5 and 10 times the segment diameter. This behavior follows from the expanded structure of the $linear_{100}$ polymer, compared to that of the more compact star polymer. The two linear polymers can relatively easily penetrate into each other, but their repulsive interaction has a longer range than that between a star-$linear_{200}$ polymer pair. Due to the globular structure of the star polymer, the penetration into the $linear_{200}$ polymer is relatively more difficult.

Figure 4 shows the radial distribution function as a function of the normalized distance between centers of mass for the $linear_{200}$-$linear_{100}$, and $linear_{200}$-star pairs for a well-depth equal to –0.40 k_BT. Radial distribution functions g_{ll} and g_{ls} appear similar. At low separations, for the star polymer it is more difficult to penetrate into the $linear_{200}$ polymer than it is for the $linear_{100}$ polymer, probably because the structure of the star polymer is more compact than that of the linear homolog.

Table 5 shows simulated osmotic second virial coefficients for the $linear_{100}$-$linear_{100}$, star-star, and $linear_{100}$-star pairs. At solvent conditions spanning from good solvents (ε=0 or ε=-0.15 k_BT) to almost theta solvents (ε=-0.30 k_BT), the osmotic second virial cross coefficient is within the osmotic second virial coefficients for the single polymers. These simulated results agree with results for linear and 8-arm star polystyrenes in toluene and cyclohexane. For a well depth –0.40 k_BT, B'_{ls} is less negative than either B'_{ll} or B'_{ss}. The weaker attraction may follow from difficulty in penetration between the two molecules due to steric effects. These simulated results roughly agree

with the experimentally measured osmotic second virial cross coefficient for linear and 8-arm star polystyrenes in methylcyclohexane, which is almost as positive as B_{ss} even though B_{ll} is negative.

Table 6 shows calculated osmotic second virial coefficients for the $linear_{200}$-$linear_{100}$, star-star, and $linear_{200}$-star pairs. At good solvent conditions (well depth equal to 0 or –0.15 k_BT), B'_{ls} is smaller than B'_{ll}. Since the radial distribution functions for the $linear_{200}$-$linear_{100}$ and $linear_{200}$-star pairs are very similar (see Figure 3), the differences between B'_{ll} and B'_{ls} are due to the different radii of gyration, which is smaller for the star polymer than for the $linear_{100}$ polymer. For a well-depth equal to –0.40 k_BT, B'_{ls} is less negative than B'_{ll}; as suggested by Figure 4, the star polymer cannot penetrate the $linear_{200}$ polymer as easily as does the $linear_{100}$ polymer.

The difference between B'_{ls} and B'_{ll} at poor solvent conditions is higher for interacting polymers of the same molecular weight because for both a flexible or a compact structure it is easier to penetrate a $linear_{200}$ polymer than a $linear_{100}$ polymer[26].

Concluding Remarks

Experimental osmotic second virial cross coefficients are reported for linear and 8-arm star polystyrenes in toluene, cyclohexane, and methylcyclohexane. The osmotic second virial cross coefficient is always positive and lies between the osmotic second virial coefficients measured for the single polymers at the same solvent conditions.

Radial distribution functions and second virial coefficients have been obtained by standard Monte Carlo simulation techniques for linear-linear, 6-arm-star-star, and for linear-6-arm-star polymers at several solvent conditions.

For polymers of comparable molecular weight at good solvent conditions the simulated second virial coefficients for non-like polymers always lie between those simulated for like polymers. However, for a well depth equal to –0.40 k_BT, B'_{ls} is less negative than either B'_{ll} or B'_{ss}.

For polymers of different molecular weight at good solvent conditions, B'_{ls} is smaller than B'_{ll} due to the different radii of gyration of the star polymers compared to those of the linear homologs. At a well depth equal to –0.40 k_BT, B'_{ls} is slightly less

negative than B'_{11} because the star polymer penetrates the $linear_{200}$ polymer less easily than does the more flexible $linear_{100}$ polymer.

Acknowledgments

This work was supported by the Director, Office of Science, Office of Basic Energy Sciences, Chemical Science Division of the U.S. Department of Energy under Contract Number DE-AC03-76SF00098. Some of the simulations were performed on a CRAY T3E supercomputer at NERSC (Berkeley, CA). The authors are grateful to Nancy Liang for assistance in experimental work and to Dusan Bratko, Robin Curtis, Camille Anderson and Ruth Wimberly for helpful discussions and encouragement.

References

1. Muthana, M.S.; Mark, H. J. Polym. Sci. 1949; 4: 527.
2. Berry, G.C. J. Chem. Phys. 1966; 44 (1-2): 4550.
3. Higo, Y.; Ueno, N.; Noda, I. Polym. J. 1983; 15 (5): 367.
4. Gauthier, M.; Chung, J.; Choi, L.; Nguyen, T.T. J. Phys. Chem. B 1998; 102: 3138.
5. Haynes, C.A.; Tamura, K.; Korfer, H.R.; Blanch, H.W.; Prausnitz, J.M. J. Phys. Chem. 1992; 96: 905.
6. George, A.; Wilson, W.W. Acta Cryst. 1994; D50: 361.
7. Guo, B.; Kao, S.; McDonald, H.; Asanov, A.; Combs, L.L.; Wilson, W.W. J. Crystal Growth 1999; 196: 424.
8. King, R.S.; Blanch, H.W.; Prausnitz, J.M. AIChE J. 1988; 34 (10): 1585.
9. Haynes, C.A.; Benitez, F.J.; Blanch, H.W.; Prausnitz, J.M. AIChE J. 1993; 39 (9): 1539.
10. Moon, Y.U.; Curtis, R.A.; Blanch, H.W.; Prausnitz, J.M. Submitted to J. Solution Chemistry, 1999.
11. Roovers, J.; Hadjichristidis, N.; Fetters, L.J. Macromolecules 1983; 16: 214.
12. Bauer, B.J.; Hadjichristidis, N.; Fetters, L.J.; Roovers, J.E.L. J. Am. Chem. Soc. 1980; 102 (7): 2410.
13. Guo, A.; Liu, G.; Tao, J. Macromolecules, 1996; 29: 2487.
14. Simms, J.A. Progress in Organic Coatings, 1993; 22: 367.
15. Likos, C.N.; lowen, H.; Watzlawek, M.; Abbas, B.; Juckischke, O.; Allgaier, J.; Richter, D. Physical Review Letters 1998; 80 (20): 4450.

16. Hiemenz , P.C.; Rajagopalan, R. Principles of Colloid and Surface Chemistry, Marcel Dekker, Inc., New York, 3rd Ed., 1997.

17. Yethiraj, A.; Hall, C.K. J. Colloid and Interface Science 1992; 151 (1): 102.

18. Meijer, E. J.; Frenkel, D. Physical Review Letters 1991; 67 (9): 1110.

19. Meijer, E. J.; Frenkel, D. Physica A 1995; 213: 130.

20. Striolo, A.; Bertucco, A.; Prausnitz, J.M. Submitted to Macromolecules, 2000.

21. Tombs, M.P.; Peacocke, A.R. The osmotic pressure of biological macromolecules, Clarendon Press, Oxford, 1974.

22. Frenkel, D.; Smit, B. Understanding Molecular Simulation, Academic Press, San Diego, 1996.

23. Allen, M.P.; Tildesley, D.J. Computer Simulation of Liquids, Oxford Science Publications, Claredon Press, Oxford, 1987.

24. Lal, M. Molecular Physics 1969; 17: 57.

25. Zifferer, G. Makromol. Chem. 1990; 191: 2717.

26. Dautenhahn, J.; Hall, C.K. Macromolecules 1994; 27: 5399.

27. Yethiraj, A.; Honnell, K.G.; Hall, C.K. Macromolecules 1992; 25: 3979.

28. Lue, L.; Prausnitz, J.M. AIChE J. 1998; 44 (6): 1455.

Table 1 Polymer properties

Polymer	Branch molecular weight g/mol	Total molecular weight g/mol	Purchased from
Linear polystyrene	-	73,000 [a]	Polymer Source, Inc.
8-arm star polystyrene	9,800	74,000 [b]	Polymer Source, Inc.

[a] from size-exclusion chromatography

[b] from light-scattering

Table 2 Solvent properties

Solvent	Purchased from	Lot number	Purity %
Toluene	Fisher Scientific	982728	99.8
Cyclohexane	Fisher Scientific	992006	99.7
Methylcyclohexane	Aldrich	LR08119KR	99

Tab. 3 Experimental osmotic second virial coefficients[1] for like and non-like linear and 8-arm star polystyrenes in different solvents. The experimental temperature is reported after each osmotic second virial coefficient. In calculating B_{ls}, for a fixed solvent, the small differences in temperature were neglected.

Solvent	B_{ll} (10^{-7} l mol / g^2)	T (°C)	B_{ss} (10^{-7} l mol / g^2)	T (°C)	B_{ls} (10^{-7} l mol / g^2)	T (°C)
Toluene	3.95±0.20	48.5	3.22±0.03	47.6	3.6±0.5	49.0
Cyclohexane	-0.12±0.01	33.8	1.5±0.3	34.2	0.15±0.3	33.7
Methylcyclohexane	-2.8±0.1	45.7	1.3±0.4	50.0	1.5±2	45.4

(1) ll = linear-linear
ss = star-star
ls = linear-star

Tab. 4 Average reduced radii of gyration squared for linear and 6-arm star polymers for different solvent conditions from molecular simulation. The reducing parameter is segment size σ.

Well depth (k_BT)	$\langle R_g^2 \rangle_{linear200}$	$\langle R_g^2 \rangle_{linear100}$	$\langle R_g^2 \rangle_{star}$
0	131±4	57±3	25±0.5[a]
-0.15	113±3	49±1	22±0.6[a]
-0.30	80±2	37±2	18.1±0.25[a]
-0.40	43.3±1.3	24.5±0.5	14.5±0.4[a]

[a] from Striolo et al.[20].

Tab. 5 Reduced osmotic second virial coefficients from molecular simulation as a function of solvent conditions. The reducing parameter is σ^3, where σ is the segment diameter.

Well depth (k_BT)	B'_{ll}	B'_{ls}	B'_{ss}
0	3027±4[a]	2730±25	2365±40[b]
-0.15	2201±2[a]	1980±40	1735±25[b]
-0.30	650±20[a]	635±20	635±3[b]
-0.40	-2600±250	-1700±150	-2070±225[b]

[a] from Dautenhahn and Hall[26].

[b] from Striolo et al.[20].

Tab. 6 Reduced osmotic second virial coefficients from molecular simulation as a function of solvent conditions. Results for non-like polymer pairs: $linear_{200}$-$linear_{100}$ and $linear_{200}$-star. The reducing parameter is σ^3, where σ is the segment diameter.

Well depth (k_BT)	B'_{ll}	B'_{ls}
0	5520±10[a]	4970±150
-0.15	4065±9[a]	3580±120
-0.30	1270±50[a]	1230±80
-0.40	-3280±400	-3020±150

[a] from Dautenhahn and Hall[26].

Figure captions

Fig. 1 Radial distribution function as a function of the distance between centers of mass, r, at athermal conditions. The distance r is normalized by the diameter of one polymer segment, σ. Diamonds represent calculations for $linear_{100}$-$linear_{100}$ polymers (from Dautenhahn and Hall[26]); squares are for star-star polymers; triangles are for $linear_{100}$-star polymers. Symbols are bigger than error bars.

Fig. 2 Radial distribution function as a function of the distance between centers of mass, r, for well depth equal to $-0.40\ k_BT$. The distance r is normalized by the diameter of a polymer segment, σ. Diamonds represent calculations for $linear_{100}$-$linear_{100}$ polymers; squares are for star-star polymers; triangles are for $linear_{100}$-star polymers.

Fig. 3 Radial distribution function as a function of the distance between centers of mass, r, at athermal conditions. The distance r is normalized by the diameter of a polymer segment, σ. Diamonds represent calculations for $linear_{200}$-$linear_{100}$ polymers (from Dautenhahn and Hall[26]); triangles are for $linear_{200}$-star polymers. Symbols are bigger than error bars.

Fig. 4 Radial distribution function as a function of the distance between centers of mass, r, for a well depth equal to $-0.40\ k_BT$. The distance r is normalized by the diameter of a polymer segment, σ. Diamonds represent calculations for $linear_{200}$-$linear_{100}$ polymers; triangles are for $linear_{200}$-star polymers.

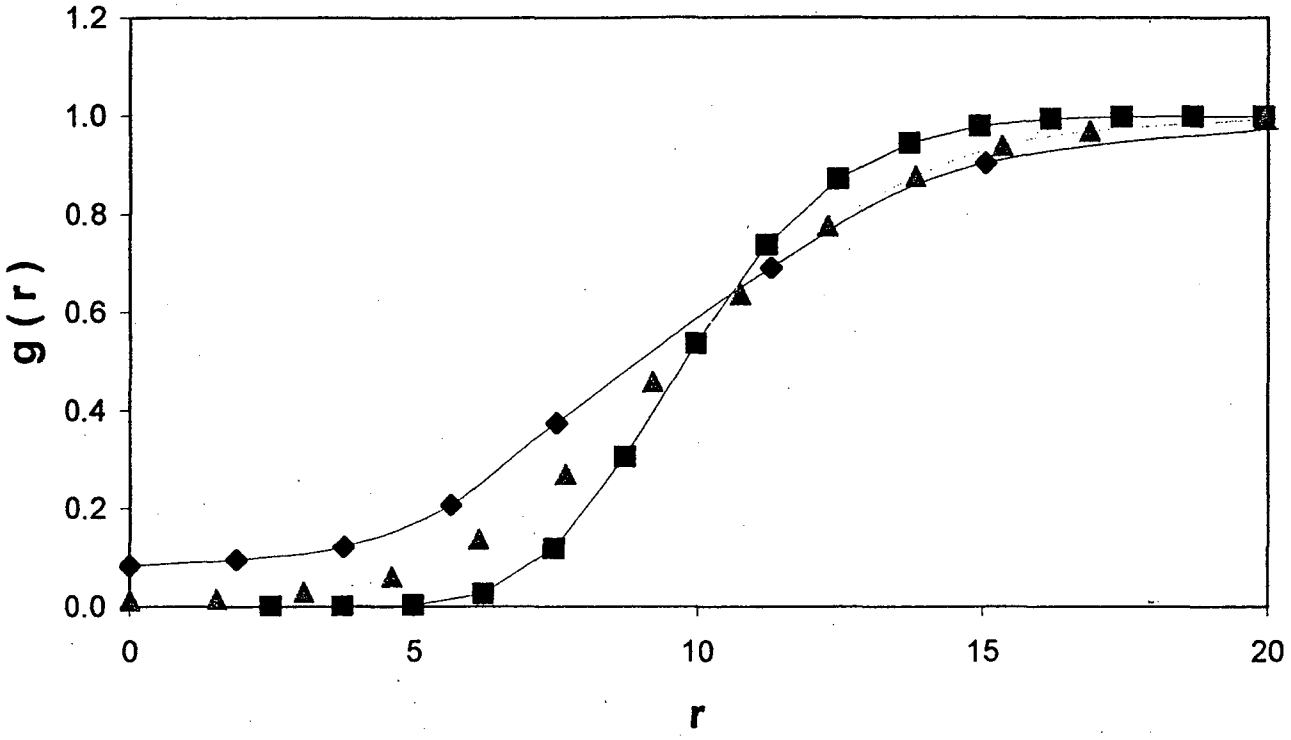

Fig. 1; Striolo et al.,

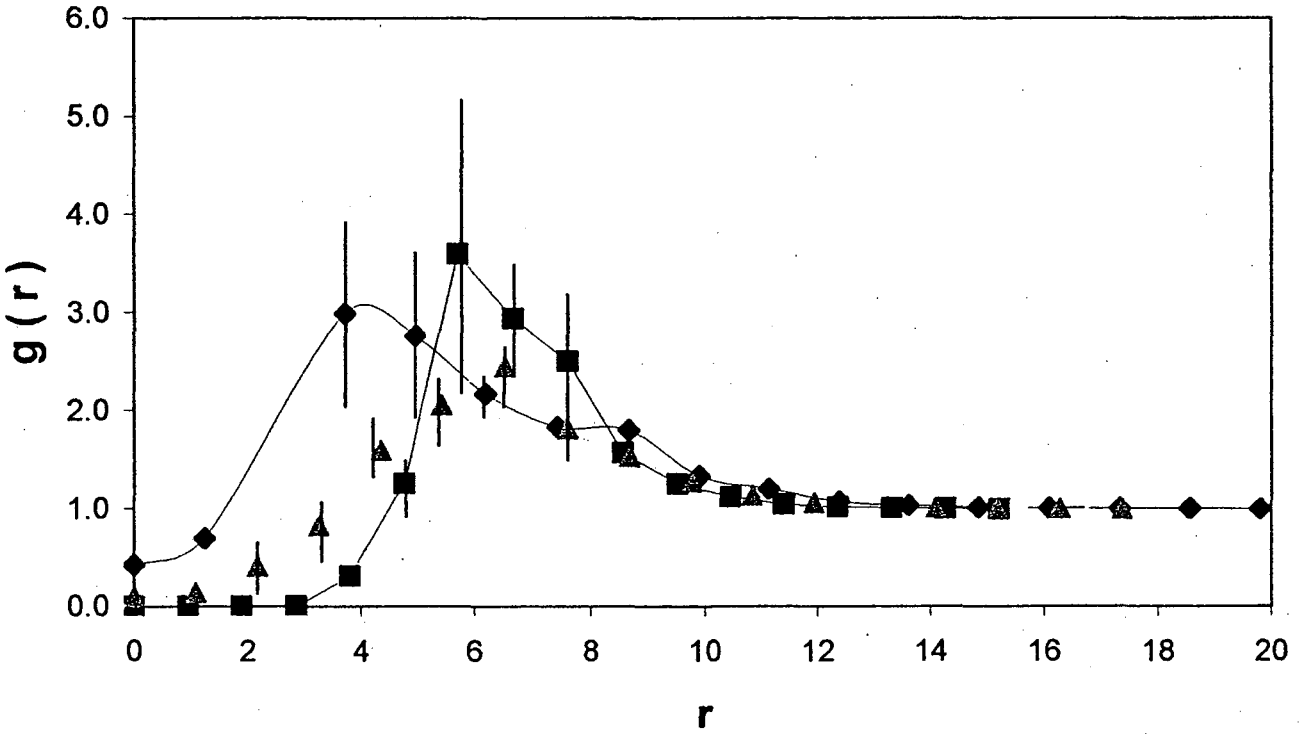

Fig. 2; Striolo et al.,

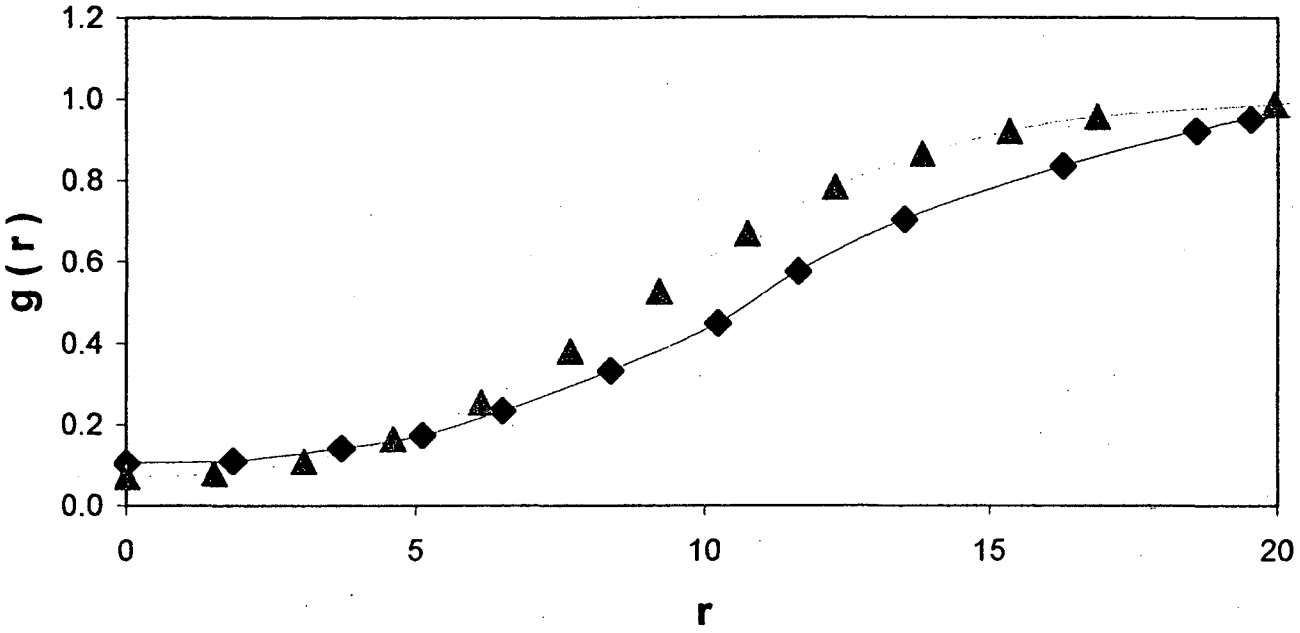

Fig. 3; Striolo et al.,

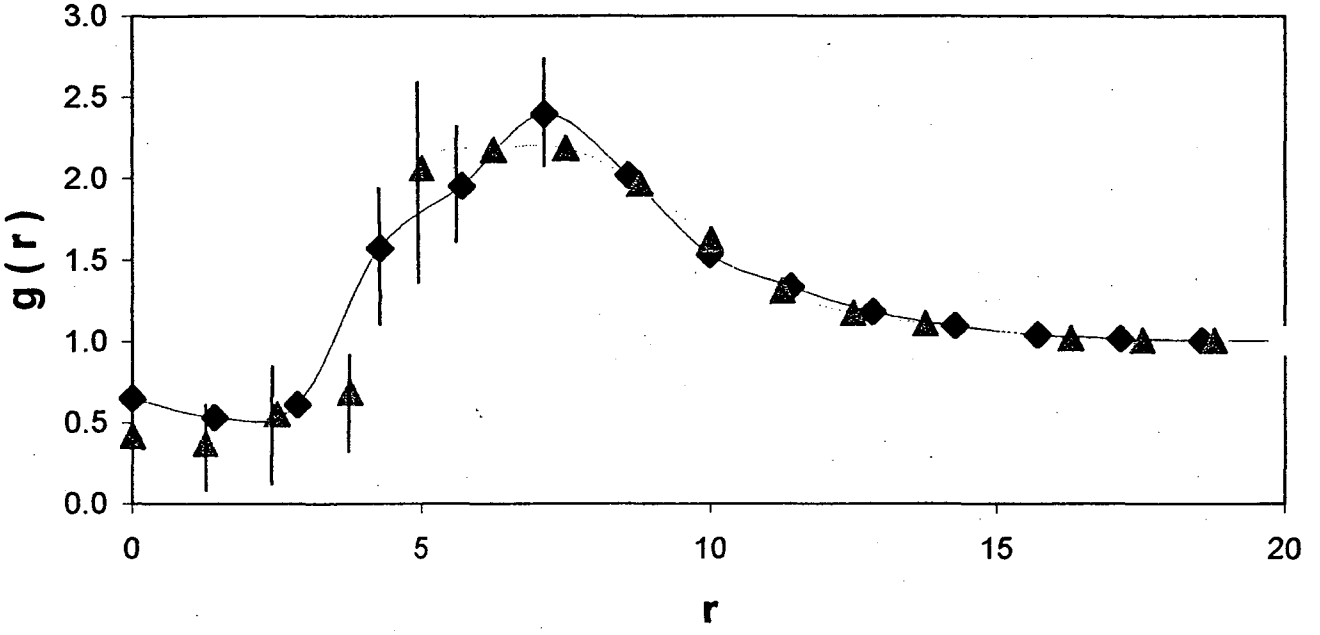

Fig. 4; Striolo et al.,

Ernest Orlando Lawrence Berkeley National Laboratory
One Cyclotron Road | Berkeley, California 94720

Prepared for the U.S. Department of Energy under Contract No. DE-AC03-76SF00098